Apoptosis-inducing factor (AIF) at the crossroad of cell survival and cell death: implications for cancer and mitochondrial diseases

Tran Ngoc Anh Nguyen, Hong-Toan Lai, Romain Fernandes, Filippo G Dall'olio, Camille Blériot, Tap Ha-Duong, Catherine Brenner

Cell Communication and Signaling

REVIEW

Open Access

Apoptosis-inducing factor (AIF) at the crossroad of cell survival and cell death: implications for cancer and mitochondrial diseases

Tran Ngoc Anh Nguyen[1], Hong-Toan Lai[1], Romain Fernandes[1], Filippo G Dall'Olio[1], Camille Blériot[1], Tap Ha-Duong[2] and Catherine Brenner[1*]

Abstract

Apoptosis-inducing factor (AIF), a mitochondrial NAD(P)H-dependent oxidoreductase, was initially studied as a cell death inducer in a process later named parthanatos. However, it has been revealed that AIF also participates in mitochondrial bioenergetics through interaction with its partner coiled-coil-helix-coiled-coil-helix domain containing 4 (CHCHD4) and involvement in mitochondrial protein import. These dual roles place AIF between pro-survival and pro-death cell fate decisions. In this review, we first describe the structure and the dual functions of AIF, highlighting its structure-function relationships. We then report previously identified *AIFM1* mutations and their clinical phenotypes. Finally, we discuss the relevance of AIF in cancer and the potential of targeting this protein for the treatment of cancer.

Keywords Apoptosis-inducing factor (AIF), Cell death, Mitochondrial protein import, Mitochondrial diseases, Cancer

Background

Mitochondria - the cellular powerhouse - have been a focus of research for nearly two centuries, yet they remain not fully understood. It has been widely accepted that mitochondria serve as a platform for metabolism and cell fate decisions. This essential organelle facilitates energy production and cellular homeostasis while continuously interacting with other compartments to orchestrate inter-organelle communication [1]. In physiological condition, the mitochondria are responsible for producing the majority of ATP required for cellular metabolism via oxidative phosphorylation (OXPHOS). In addition, parts of lipid and pyrimidine metabolisms occur within the mitochondria, and these organelles also regulate the levels of amino acids [2]. In addition to their involvement in metabolism, the mitochondria physically communicate with other intracellular compartments through the outer mitochondrial membrane (OMM), such as the nucleus, endoplasmic reticulum (ER), peroxisomes and lysosomes, thus contributing to numerous processes including signal transduction, calcium homeostasis, vesicle transport, and stress response [2]. This crosstalk with other organelles further highlights the importance of mitochondria in cellular homeostasis by ensuring optimal functions, metabolism, growth and survival. Moreover, their roles

*Correspondence:
Catherine Brenner
catherine.brenner@gustaveroussy.fr
[1]Aspects métaboliques et systémiques de l'oncogénèse pour de nouvelles approches thérapeutiques, CNRS, Institut Gustave Roussy, Université Paris- Saclay, Villejuif, France
[2]BioCIS, CNRS, Université Paris-Saclay, Orsay 91400, France

also extend beyond the cellular level, impacting the physiology of the entire organism by modulating interactions between cells and tissues [2]. As the mitochondrial genome is a small circular genome that encodes for only 13 proteins [3] to ensure the correct functions of mitochondria, the majority of mitochondrial proteins are encoded in nucleus and transported into mitochondria. Of note, mitochondrial genetic defects can lead to complex diseases and affect mostly neurological and muscular functions. The biggest challenge in treating mitochondria-related diseases is the extremely varied genotype-phenotype relationship [4]. This highlights the important role of mitochondria in maintaining the intricate structure and function of the whole human body.

Beyond their widely recognized roles in energy metabolism, reactive oxygen species (ROS) regulation, calcium signaling and cellular homeostasis, the mitochondria are involved in different cell death pathways, notably apoptosis. Apoptosis is a form of regulated cell death that plays a key role in maintaining life/death balance by eliminating damaged, infected and/or cancerous cells [5]. Many apoptosis-targeting drugs have demonstrated remarkable clinical efficacy and are being used to treat various diseases. For example, the success of Venetoclax, an anti-apoptotic Bcl-2 inhibitor, has been evident in the treatment of chronic lymphocytic leukemia and acute myeloid leukemia [6]. Historically, mitochondria-dependent apoptosis was associated with mitochondrial outer membrane permeabilization (MOMP) induced by pro-apoptotic Bcl-2 family proteins, and consequently cytochrome c (Cyt c) release and Apaf-1-mediated activation of caspases [7]. In addition to Cyt c, other mitochondrial proteins have been identified as cell death regulators, including endonuclease G (EndoG), Smac/DIABLO, Omi/HtrA2, and Apoptosis-Inducing Factor (AIF) [8]. Unlike Cyt c, AIF mediates caspase-independent cell death, later designated as parthanatos [9, 10].

The *AIFM1* gene is located in X chromosome and encodes for protein precursor that later undergoes proteolytic cleavage to form AIF with pro-death activity [11]. Therefore, mitochondrial dysfunction in a wide range of human pathologies, such as ischemia-reperfusion injury, neurodegeneration, or cancer, could be attributed to this property of the protein [12, 13]. However, interestingly, more recent studies have discovered the pro-survival endogenous properties of AIF, revealing the complex nature of this protein. Thus, as an oxidoreductase, AIF contributes indirectly to various mitochondrial activities, especially via the biogenesis of respiratory chain complexes. These functions are linked to the binding of AIF to its partner Coiled-Coil-Helix-Coiled-Coil-Helix Domain Containing 4 (CHCHD4), thus modulating the import of different mitochondrial protein subunits [14]. This discovery places AIF at the crossroad between pro-survival and pro-death cell decisions, both in physiological and pathological conditions.

Despite numerous reviews about the physiological roles of AIF, its contradictory, yet fascinating position between pro-death and pro-survival is a hot topic of interest in a therapeutic perspective. Therefore, this review first explores the structural organization of AIF, which dictates its multiple subcellular localization and dual functions. Then, we will also examine human pathologies induced by mutations in *AIFM1* with different reported clinical cases, thus demonstrating a link between genotype and phenotype. Finally, we will provide an overview of AIF's involvement in cancer, as well as the emerging potential of AIF-targeting therapies for cancer treatment.

AIF: primary structure and versatile functions

The AIF precursor (67 kDa) is encoded in the nucleus and consists of six regions: mitochondrial localization sequence (MLS) (residues 1–53/54), intermembrane sequence (residues 66/67–84/85), two FAD-binding domains (residues 128–262 and 401–480) framing one NAD(P)H-binding region (residues 263–400), and C-terminal (residues 481–613) (Fig. 1) [11, 15]. Comparison of the backbones of AIF, *Pseudomonas sp.* ferredoxin reductase component BphA4, and *Escherichia coli* glutathione reductase revealed high structural similarity, except for the C-terminal regulatory loop (residues 509–559) absent in the other two proteins [15, 16]. This region contains a Pro/Glu/Ser/Thr (PEST)-rich sequence and a Pro-rich motif, both of which are involved in protein-protein interactions. Alignment of human and mouse AIF amino acid sequences demonstrated an identity of 92%, which correlates with high structural similarity [10, 15, 16]. It has been reported that at least 40 first residues of the N-terminal were required for mitochondrial localization of AIF. Upon mitochondrial import, the AIF precursor is then cleaved at position Met53/Ala54 by mitochondrial processing peptidase (MPP), eliminating the MLS. The adjacent intermembrane sequence contains hydrophobic residues 66–84 and assists in the sorting and insertion of mature AIF (62 kDa) into the inner mitochondrial membrane (IMM), facing the intermembrane space (IMS) [11].

After being inserted in the IMM, three modifications of AIF allow for its functional maturation.

Flavin adenine dinucleotide (FAD) association

First, the incorporation of the cofactor FAD is required to establish AIF oxidoreductase activity. Thus, the adenine nucleoside and pyrophosphate group of FAD interacts with the FAD-binding domain of AIF, while the isoalloxazine ring is partially exposed as the redox center [15].

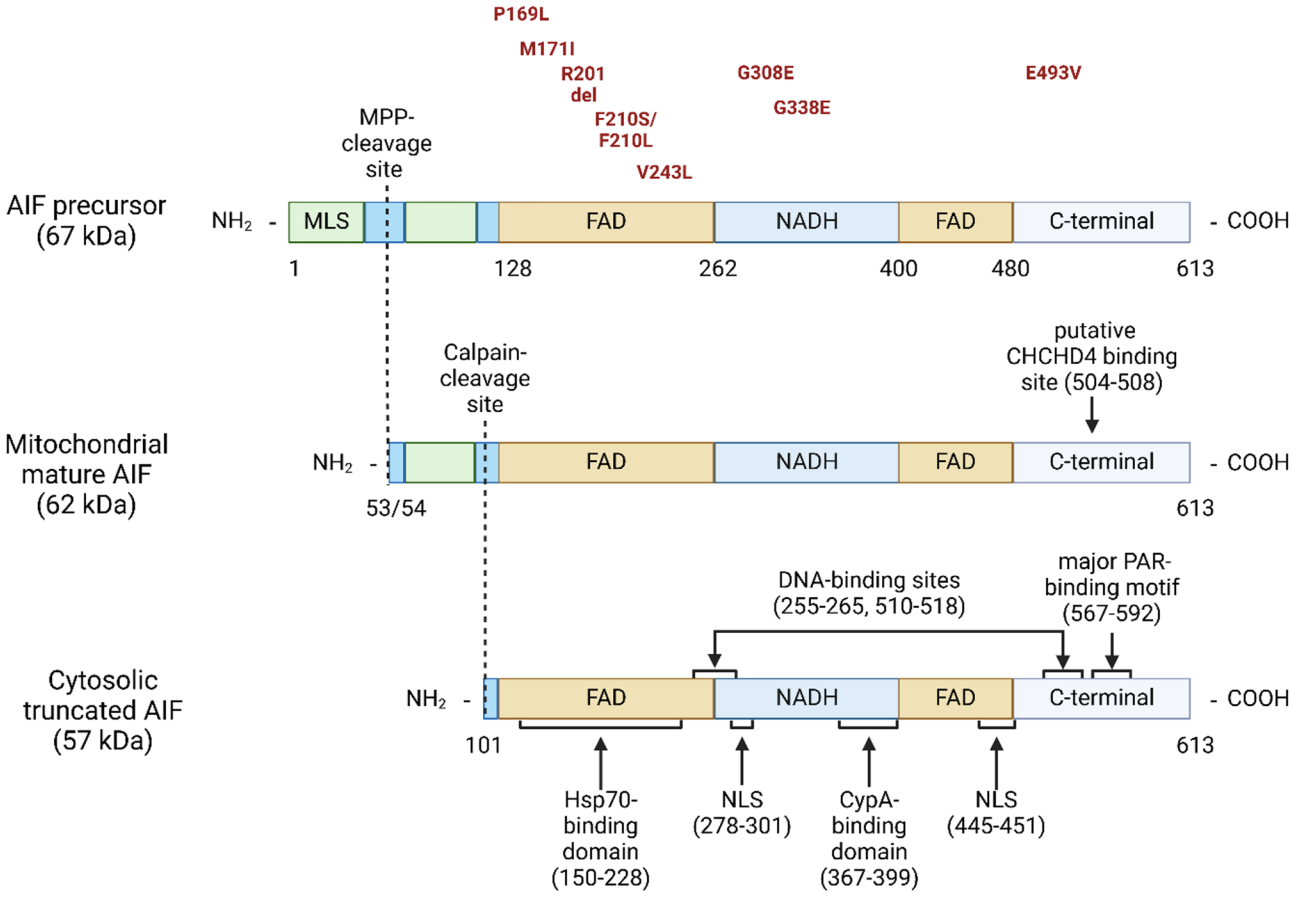

Fig. 1 Schematic illustration of different structural domains in AIF precursor, mitochondrial mature AIF and cytosolic truncated AIF. Clinically relevant AIF variants discussed in this review are highlighted in red. MLS, mitochondrial localization sequence; MPP, mitochondrial processing peptidase; PAR, Poly(ADP-Ribose); Hsp70, Heat-shock protein 70; CypA, Cyclophilin A; NLS, nuclear localization sequence

Reduced nicotinamide adenine dinucleotide/reduced nicotinamide adenine dinucleotide phosphate (NADH/NADPH) binding

Homology has been found between AIF and NADH-dependent ferredoxin reductase from bacteria and archaebacteria, as well as yeast NADH-dependent ubiquinone oxidoreductase, which further suggests the NAD(P)H-dependent enzymatic activity of the protein [15, 16]. Reduction with NAD(P)H results in significant reorganization of AIF, facilitating the formation of dimeric, stable $FADH_2$-NAD + charge-transfer-complex (CTC). Therefore, the equilibrium of monomeric/dimeric AIF likely depends on the incorporation of NAD(P)H. In addition, kinetic measurements demonstrated that AIF had a 100-higher fold preference for NADH compared to NADPH, and reaction of the protein with NADPH occurred at a slower rate [17]. Structural analysis of reduced, NAD-bound Δ1–101 AIF purified from E. coli showed FAD in the 2-electron reduced state, and the two monomers positioned close together with a network of both hydrophobic and polar bonds [18]. At the active site, the nicotinamide ring of NAD(P) and the isoalloxazine ring of the reduced flavin ($FADH_2$) stack closely together, which allows for electron transfer [17, 18]. Reduction with NAD(P)H also induces movement of residue His453 at the second FAD-binding domain, which orients NAD for charge transfer. The involvement of His453 has been further confirmed by the inability of the His453Leu AIF variant to form CTCs [17].

C-terminal conformation

Other significant conformational changes occur at the C-terminal, including formation of an aromatic tunnel connecting the active site to the surface of the protein that assists in electron transfer, as well as dislocation of the entire regulatory peptide (residues 509–559, C-terminal). These changes further result in exposure of Thr195 of the β-hairpin (residues 190–202, first FAD-binding domain) into the solvent, potentially regulating the rate of electron and radical exchange with partners of AIF [18].

During AIF-dependent cell death, IMM-bound AIF is processed into a soluble form that can be released into the cytoplasm. Study of different truncated AIF variants

revealed that the N-terminal sequence between residues 96 and 110 was involved in this cell death-induced release, and the protein was likely cleaved at position 101 (Fig. 1) [11]. Thus, following permeabilization of the OMM, truncated AIF translocates to the cytoplasm, where its fate depends on interactions with different partners at specific binding regions. To execute its function in cell death, AIF finally reaches the nucleus, binds directly to DNA and triggers chromatin condensation [10, 16].

Interestingly, the incorporation of NAD(P)H has been suggested to inhibit AIF/DNA interaction. To demonstrate this phenomenon, Churbanova et al. performed an electrophoretic migration assay, in which DNA was pre-incubated with truncated Δ1–101AIF in the presence of NAD(P) or NAD(P)H. Unlike NAD(P), the addition of NAD(P)H did not reduce the motility of DNA in the gel, indicating that there was no binding of AIF to DNA [17]. One possible explanation as to why reduction with NAD(P)H negatively affects AIF/DNA interaction could lie in the redox-induced dramatic changes in the regulatory peptide (residues 509–559, C-terminal), which contains elements critical for DNA binding. In more details, the affinity of AIF to DNA might be influenced by positioning of residues Leu510 and Leu518, along with folding of the 509–517 segment [16, 18]. Another explanation would be the inaccessibility of nuclear leading sequence (NLS) positioned at residues 445–451 in dimeric, reduced AIF, which lowers the ability of CTC to translocate to the nucleus and induce cell death [18].

In addition to proteolytic cleavage during IMM insertion and nuclear translocation, as well as redox changes, AIF is also subjected to other post-translational modifications including ubiquitination, deubiquitination, and phosphorylation. It has been shown that interaction with X-linked inhibitor of apoptosis (XIAP) induces ubiquitination of AIF, more specifically under cell death conditions. Moreover, plasmid co-expression of XIAP and mature (62 kDa) or truncated (57 kDa) AIF resulted in lower basal and antimycin A-induced ROS levels, compared to control. Thus, the XIAP/AIF complex contributed to ROS regulation without inducing proteasomal degradation of AIF or altering XIAP-mediated caspase inhibition [19]. In agreement with this study, Lewis et al. also demonstrated that AIF ubiquitination by XIAP was nondegradative, and further experiments revealed Lys255 as the site of ubiquitination. As mutation of this residue diminished the DNA binding activity of AIF and interfered with AIF-dependent chromatin degradation, it was concluded that XIAP directly affects AIF cell-death inducing capacity [20]. On the contrary, deubiquitination at Lys255 by OTU deubiquitinase 1 (OTUD1) was shown to enhance binding of AIF to DNA and AIF-dependent cell death. Interestingly, OTUD1 also mediated AIF deubiquitination at Lys244, which led to abnormal mitochondrial ultrastructure (swollen mitochondria without intact cristae), compromised OXPHOS and induced a glycolytic switch [21]. Besides ubiquitination and deubiquitination, AIF also undergoes phosphorylation. In a study by Xing et al., AIF was demonstrated to interact with p21 activated kinase 5 (PAK5) at residues 263–480. Further analysis revealed that the resulting phosphorylated AIF at Thr281 exhibited decreased nuclear translocation due to diminished binding with nuclear importin α3 [22]. It can be seen that these changes in AIF influence its functions in the cell; however, more study is needed to explore other post-translational modifications. To sum up, the structure and functions of AIF could vary depending on its subcellular localization, binding of the cofactor FAD, redox state, interactions with partners, and post-translational modifications.

AIF as a cell death effector: nuclear translocation and parthanatos

AIF nuclear translocation

As indicated by its name, human AIF was discovered by Susin et al. for its implication in caspase-independent cell death [10]. To fulfil this role, following MOMP, truncated AIF (57 kDa) is released from the mitochondria, accumulates in the cytosol and translocates to the nucleus (Fig. 2A). Initially, molecular characterization of AIF demonstrated that the protein was confined to the mitochondria in healthy cells and translocated to the cytosol and nucleus after treatment of these cells with the apoptosis inducer staurosporine [10].

Release to the cytosol

The release of IMM-bound AIF requires its cleavage at position 101 by cytosolic or mitochondrial proteases [11]. Several studies have shown that calpains are responsible for this cleavage. Calpains are calcium (Ca^{2+})-activated cysteine proteases that also process members of the Bcl-2 family of cell death regulators such as Bid. In isolated mitochondria of mouse liver and brain, treatment with calpain I and Bid strongly induced AIF release, which was reversed after addition of a calpain inhibitor. This release was reported as Ca^{2+}-mediated, and the enzyme could cleave recombinant AIF and potentially liberates the protein from the IMM [23]. Another study demonstrated similar enzymatic activity of calpain on AIF in the context of ischemic neuronal injury. In a cell-free assay in which mature AIF (62 kDa) was incubated with different cysteine proteases including calpains, caspases and lysosomal cathepsins, only calpain I was recorded to produce a specific fragment of AIF at 57 kDa. In addition, site-directed mutagenesis at position 100–103 completely abolished calpain-dependent cleavage, confirming the residues involved. Further in vitro

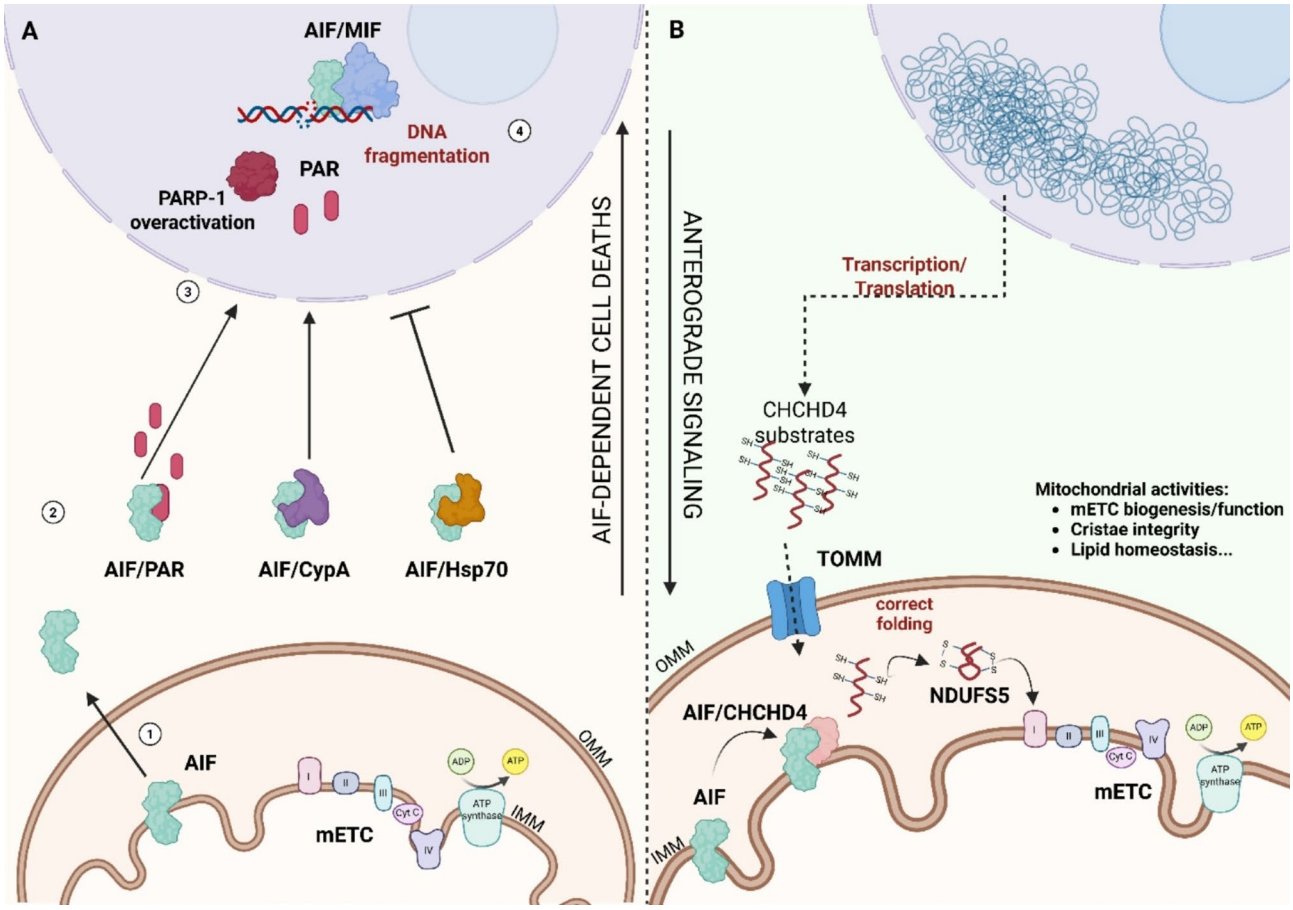

Fig. 2 The dual roles of AIF in cell death and in vital mitochondrial functions. (**A**) In AIF-dependent cell death, AIF is released from the mitochondria, translocates to the cytosol (step 1) and binds to protein partners and parthanatos-associated PAR induced by PARP-1 overactivation (step 2), which facilitates its nuclear entry (step 3). Once inside the nucleus, AIF works with endonucleases and mediates DNA degradation (step 4). (**B**) On the contrary, pro-survival roles of AIF rely on its interaction with CHCHD4 and involvement in the CHCHD4-dependent mitochondrial import pathway of nuclear-encoded cysteine-rich substrates. Thus, AIF contributes to anterograde signaling pathway from the nucleus to mitochondria. Here, particularly illustrated in the figure is the correct folding and retention of NDUFS5, a subunit of complex I in the mETC. Other mitochondrial activities relevant to AIF/CHCHD4 interaction are mentioned by text. mETC, mitochondrial electron transport chain; PAR, Poly(ADP-Ribose); Hsp70, Heat-shock protein 70; CypA, Cyclophilin A; PARP-1, poly(ADP-ribose) polymerase-1; MIF, macrophage migration inhibitory factor; OMM, outer mitochondrial membrane; IMM, inner mitochondrial membrane. The figure was adapted from Reinhardt et al. [48]

experiments concluded that calpain I activation was necessary and sufficient to induce AIF truncation and release in oxygen-glucose deprived neurons [24].

Interactions with cytosolic proteins and entry into the nucleus

After its cleavage and release from the mitochondria, cytosolic AIF interacts with other proteins including heat shock protein 70 (Hsp70) and cyclophilin A (CypA), which regulate its translocation to the nucleus. While Hsp70 is antagonistic and prevents AIF from nuclear entry, CypA promotes this process. Ravagnan and coll. showed that Hsp70 exhibits direct binding to AIF, evidenced by ligand blotting and co-immunoprecipitation. Moreover, stable overexpression of Hsp70 minimized cell death, coincidental with increased Hsp70-AIF interaction, while downregulation of Hsp70 showed the reverse effects [25]. AIF was also reported to interact with CypA, however at different residues from the Hsp70-binding domain. The AIF-CypA complex exhibited greater capacity to induce chromatin degradation compared to either protein alone, seen in isolated nuclei, purified DNA and intact cells [26]. In another study using cerebral hypoxia-ischemia as a model, AIF was confirmed to bind directly to CypA, and this interaction was found to be essential for nuclear translocation of AIF [27]. In addition to interacting with its partners, it is possible that AIF also relies on the NLS for nuclear entry, which is positioned in the NADH-binding domain (residues 278–301) and the second FAD-binding domain (residues 445–451). Further study is required to conclude whether this process is active and requires the use of ATP. Moreover, since diminished ATP production is common during cell death due to disrupted mitochondrial electron transport chain

(ETC) [28] an increase in permeability of the nuclear pore complex might be sufficient for translocation of AIF. For example, in excitotoxic neuronal death, degradation of nuclear pore complex components was reported to alter the permeability of the nuclear membrane, thus mediating the redistribution of proteins such as AIF in the nucleus [29].

Truncated AIF in the nucleus

Inside the nucleus, direct binding of AIF to DNA is required for the cell death-inducing property of the protein, which is characterized by DNA fragmentation of 20 to 50-kb and subsequent chromatin condensation. Moreover, AIF translocation was reported to coincide with a reduction in mitochondrial membrane potential and chromatin condensation in the nucleus using MitoTracker Red and Hoechst fluorescent probes staining, respectively. When added on nuclei of HeLa cells, recombinant AIF induced DNA loss and chromatin condensation, further confirming the apoptogenic activity of the protein [10]. Another study reported similar observations, in which AIF entered the nucleus and partially co-localized with condensed chromatin during staurosporine-induced early apoptosis. However, in the next stage of chromatinolysis and formation of apoptotic bodies, this association was no longer recorded, indicating the role of AIF as an early cell death effector. Mutations at different positively charged positions of AIF reduced its affinity to DNA, and mapping of these residues suggested a possible DNA-interacting region. More notably, the effects of these mutants on DNA binding capacity correlated with their ability to induce cell death [16]. In addition, as previously described, the apoptosis-inducing effects of AIF do not require reduction with NAD(P)H, which highlights the structure-function relationship of the protein, and its distinct roles in redox activity and induction of cell death [17]. As AIF does not possess intrinsic nuclease property, it is likely that the protein could recruit other endonucleases for DNA degradation. In *C. elegans*, the orthologs of AIF (WAH-1) and endonuclease G (CPS-6) were reported to interact and induce chromatin fragmentation, defining a possibly conserved mitochondria-originated DNA degradation machinery [30]. However, there has been evidence suggesting that EndoG is likely not involved in AIF-dependent DNA degradation in mammalian cells, and the macrophage migration inhibitory factor (MIF) might be a direct nuclease partner of AIF [13]. In this study, AIF was shown to interact with MIF in pulldown analysis and MIF mediated its translocation to the nucleus in cortical neurons and HeLa cells treated with N-methyl-D-aspartate (NMDA) and N-methyl-N′-nitro-N-nitrosoguanidine (MNNG). Accordingly, *MIF* knockout cells transduced with AIF binding-deficient MIF mutant demonstrated no obvious large DNA fragmentation and resistance to AIF-induced cell death. Similar observations were reported in vivo, confirming the essential role of AIF/MIF interaction in the induction of DNA damage and cell death.

AIF in parthanatos

The cell death pathway involving AIF is later designated as parthanatos, showing characteristics different from other forms such as apoptosis, necrosis or autophagy [9]. Cellular consequences of parthanatos include phosphatidylserine flipping on the plasma membrane, mitochondrial membrane depolarization, large DNA fragmentation, and chromatin condensation. In mouse embryonic fibroblasts treated with MNNG, AIF translocation, nuclear condensation, and dissipation of the mitochondrial membrane potential were reported within 15 min, followed by Cyt *c* release after 1–2 h [31]. Molecularly, parthanatos is distinguished by an overactivation of poly(ADP-ribose) polymerase (PARP) [32]. PARPs are nuclear enzymes that respond to DNA damage and contribute to DNA repair. However, the overactivation of PARPs induces poly(ADP-ribose) (PAR) synthesis and accumulation, which is involved in cell death such as seen in cerebral ischemia, neurodegenerative diseases, and heart attack [12, 13]. Interestingly, knock-out (KO) of *PARP-1* in fibroblasts and cortical neurons diminished AIF translocation to the nucleus, concomitant with loss of PAR production and failure to elicit nuclear condensation or cell death, compared with WT cells. Moreover, these effects could not be alleviated by treatment with caspase inhibitors, confirming that parthanatos is caspase-independent [31]. The mechanism of which PARP-1 overactivation and PAR production eventually leads to AIF release from the mitochondria has been extensively explored. PAR was reported to physically bind to AIF in both cell-free assay and intact cells, and their interaction increased significantly after treatment with cell death inducers. Moreover, the same study identified a PAR-binding motif (PBM) on the sequence of AIF, with putative, evolutionarily conserved sites at 222–244, 441–463 and 567–592. Moreover, peptide binding and mutational analysis confirmed residues 567–592 at the C-terminal of AIF as the major PBM, without excluding other sites, separable from the DNA-binding domain of the protein. AIF mutant in the PBM region-maintained PAR-independent properties including NADH oxidase activity and FAD binding in cell-free assays, as well as DNA binding and induction of chromatin condensation and nuclear shrinkage in isolated nuclei. However, this mutation diminished AIF/PAR interaction, release of the protein from the mitochondria, translocation to the nucleus, and ability to induce parthanatos both in vitro and in vivo [33].

AIF-dependent induction of cell death involves intricate processing of the protein, from correct cleavage and

release from the mitochondria, interaction with PAR, CypA and Hsp70, direct binding to DNA, to finally execution of DNA degradation with potential endonucleases. Interestingly, AIF has been shown to be indispensable for programmed cell death (PCD) during embryogenesis. *AIF*-ablated murine embryonic stem cells (ESCs) were unable to generate chimaeric mice when injected into blastocysts yet maintained the capacity to differentiate into cells of all three germ layers. Further investigation revealed that $AIF^{-/Y}$ ESCs exhibited a block in cavitation, as ectodermal cells in the inner core of embryoid bodies failed to undergo PCD. Moreover, PCD of the inner cells was independent of the Cyt *c*/ Apaf1/ caspase 9 apoptosome, and translocation of AIF from mitochondria to the nucleus was observed [34]. Relevant to these findings of AIF's role in embryogenic development, there have not been in vivo models of *AIFM1* knockout, and most studies of AIF deficiency have utilized the Harlequin (Hq) mouse. These mice carry a proviral insertion in the *AIFM1* locus and exhibit up to 80% loss of the protein [35]. Neuronal cultures from harlequin (Hq) mice demonstrated a reduction in DNA fragmentation, loss of mitochondrial polarization, and resistance to death induced by the DNA damaging molecule camptothecin when compared to WT cells [36]. In addition, the lethal function of AIF has also been implied in many human pathologies such as cerebral hypoxia-ischemia, myocardial ischemia, and cancer [27, 37–39]. Further study is required to define the whole dynamic AIF interactome involved in cell death, and to elucidate the exact mechanisms by which AIF contributes to the onset of different pathological conditions.

Considering the roles of AIF in parthanatos, it is possible to speculate about compounds that exploit this process for cancer treatment. Indeed, oxaliplatin, a platinum chemotherapeutic agent, has been shown to trigger cell death in oral squamous cell carcinoma (OSCC) through an AIF-dependent mechanism [40]. In vitro, oxaliplatin exhibited time- and dose-dependent induction of cell death and suppression of OSCC clonogenic capacity and migration, as well as depolarization of the mitochondrial membrane. Protein expression levels of parthanatos cascade members PARP-1, AIF and MIF were upregulated in the nucleus of oxaliplatin-treated cells compared to the control, concomitantly with increased translocation of AIF to the nucleus reported by immunofluorescence. Co-treatment of cells with a PARP-1 inhibitor reversed all effects of oxaliplatin, confirming its ability to mediate cell death, mainly via parthanatos. Moreover, antioxidant-mediated mitigation of ROS production significantly reduced parthanatos in oxaliplatin-treated cells, which suggested a possible link between ROS and parthanatos [40]. Similar observations were reported after treatment of eosophageal cancer cell lines with the transcriptional repressor of survivin, YM155. YM155 triggered non-apoptotic, caspase-independent death in these cells, together with PARP-1 and PAR accumulation and AIF translocation to the nucleus. In addition, microarray analysis revealed changes in the transcription levels of active PARP-regulated, but not necrotic or apoptotic genes, further highlighting the involvement of parthanatos in YM155-induced cell death [41]. Mono- and combination- treatments with various other drugs have also been demonstrated to induce PARP-1 upregulation, accumulation of PAR, and AIF translocation from mitochondria to the nucleus, eventually leading to AIF-dependent death in breast cancer, liver cancer, glioma, mantle cell lymphoma and acute T-cell leukemia cell lines [42–47]. While AIF-mediated parthanatos induced by some of these compounds might be associated with excessive ROS production, oxidative stress, and c-Jun N-terminal protein kinases (JNK) activation [40, 44–46] in-depth investigation is necessary to fully elucidate the upstream and downstream processes modulating this cell death pathway and to harness it for the development of novel anticancer therapies.

More than cell death: aif's role in anterograde signaling pathway

Beyond parthanatos, speculation about the role of AIF in mitochondrial bioenergetics was raised after analysis of the characteristics of Hq mice and finally led to the notion that AIF is involved in the so-called anterograde signaling pathway that governs the flow of proteins and information from the nucleus to mitochondria [49]. This pathway functions through the activation of nuclear transcription and cytoplasmic mRNA translation which directly regulate mitochondrial biogenesis.

As previously reported by Klein et al., the Hq mice exhibited progressive degeneration of differentiated cerebellar and retinal neurons, accompanied by increased oxidative stress and aberrant re-entry in the cell cycle [35]. In addition to the brain and retina of Hq mice, effects of AIF deficiency have been examined in skeletal muscles. Hq mice demonstrated lower muscle mass and atrophic myofibers without signs of apoptosis, necrosis or autophagy. Further analysis detected delayed skeletal regeneration, DNA damage, and oxidative stress in these cells, which might expand the role of AIF to protection against oxidative damage to DNA [50]. Involvement of AIF in the modulation of ROS was also reported in thymocyte maturation. More specifically, AIF deficiency increased ROS production and oxidative stress-induced apoptosis in thymocytes of Hq mice, which correlated with the reduction in cell number as well as impaired T lineage cell development [51]. However, despite the effects of AIF downregulation on oxidative stress, there has not been sufficient evidence suggesting that the

protein directly modulates ROS or scavenges free radicals so far.

Since neurodegeneration and retinal degeneration are common symptoms of OXPHOS defects, an aberrant cell death mechanism or increased oxidative stress could be insufficient or irrelevant to what was observed in Hq mice. Therefore, to investigate the putative role of AIF in mitochondrial bioenergetics, Vahsen et al. have studied AIF-deficient (AIF–/y) ESCs in addition to Hq mice [52]. In these cells, a significant decrease in complex I-dependent substrate oxidation was reported, in alignment with a defect in enzymatic activity, without changes in other complexes of OXPHOS. In addition, the cells showed decreases in the protein expression level of subunits of complex I, and to a lesser extent complex III, without evidence for mitochondrial DNA depletion or gross mitochondrial biogenesis disruption. Metabolically, AIF deficiency switched the cells to a more glycolytic phenotype compared to the control cells. Similar findings on complex I were demonstrated in mitochondria collected from the brain and retina, but not from the heart or liver of Hq mice, indicating that AIF downregulation-associated complex I deficiency was found only in affected organs. Following this discovery of the involvement of AIF in OXPHOS, more research has been conducted on the whole brain of Hq mice, including different cell populations and throughout disease progression, as a validation of this in vivo model to study complex I-deficient disorders [53]. On a larger scale, it has been demonstrated that the activity of complex I varied among different organs of Hq mice, with retina (75% loss) and brain (40% loss) as the most affected. Slightly decreased activity was seen in the spinal cord, kidney, and skeletal muscles, despite no changes reported for the heart, liver, or testis. Interestingly, strong correlation was found between complex I activity and the protein expression level of its subunit NDUFB8 [54]. These findings emphasize the cell-type specific vulnerability to AIF deficiency, as well as the effects on complex I expression and activity. However, more detailed studies are required to understand the mechanisms behind these observations.

It has been demonstrated that lower protein expression of complex I subunit in *AIF*-knocked-out ESCs is not due to reduced mRNA levels, suggesting that AIF might contribute to the post-transcriptional biogenesis of the respiratory complex [52]. The protein was later identified as a direct binding partner of CHCHD4, which provides an insight into its participation in respiratory chain biogenesis through the CHCHD4-dependent mitochondrial import pathway (Fig. 2B) [14]. In this study, AIF carrying a clinically pathological mutation that results in severe complex I and IV deficiency showed a reduction in CHCHD4 binding, highlighting the potential relationship between AIF/CHCHD4 interaction and the activity of these complexes. To further explore the implication of CHCHD4 in respiratory chain biogenesis, CHCHD4-deficient embryos and cells were generated, both of which exhibited reduced protein expression of subunits in complex I and IV, corresponding to their defective activities. Interestingly, AIF downregulation resulted in similar findings, accompanied by a decrease in CHCHD4 protein expression without changes in its mRNA level. By fusing CHCHD4 with the MLS of AIF, the authors reversed the phenotypes previously recorded in AIF-deficient cells. Thus, it was concluded that the involvement of AIF in OXPHOS might be mediated through AIF-dependent import of CHCHD4 and its direct interaction with CHCHD4. Interestingly, although Hangen et al. demonstrated a decrease in CHCHD4 protein level after AIF knock-down in U2OS cell line [14] it was reported that CHCHD4 protein expression in *AIFM1* knockout HEK293 cells remained unchanged, and only shifted the balance towards monomeric, soluble CHCHD4 that was unbound with AIF [55]. This discrepancy might be due to different cell models and methods of inducing AIF deficiency (knockout vs. knockdown), as well as possible mechanisms to avoid proteasomal degradation of cytosolic CHCHD4 precursor [56]. Nevertheless, these observations have highlighted the relevance of AIF in maintaining the expression and the structural state of CHCHD4. Formation of long-lived AIF/CHCHD4 complex was later confirmed and also revealed a stoichiometry of two AIF molecules to one CHCHD4 molecule [55, 57]. In addition, the presence of NAD(P)H was shown to enhance the binding between the two proteins, suggesting the redox state-dependent nature of this interaction [14, 55, 57]. In agreement with available experimental data [14, 55] 3D modelling and coevolution analysis indicated an interaction between 27 N-terminal residues of CHCHD4 and the C-terminal of AIF, mainly at residues 504–508 [58]. Recently, reduction with NADH was demonstrated to stimulate the formation of AIF/CHCHD4 complex, through release of AIF's regulatory peptide (also known as the C-loop, residues 509–559 of the C-terminal). Further analysis on crystallized structures of the AIF/CHCHD4 interaction in excess NADH showed one or two CHCHD4 bound to a single AIF dimer, and CHCHD4 to hydrophobically scaffold the exposed C-terminal of AIF. NADH-activated, CHCHD4-bound AIF then regulated the access to the active site of CHCHD4 and enhanced its function of substrate refolding and disulfide formation [57].

In addition to subunits of OXPHOS complexes, CHCHD4 is essential for the import of other nuclear-encoded cysteine motif-carrying proteins into the mitochondrial IMS. Understanding of human CHCHD4 has come from extensive studies on its yeast ortholog Mia40, with evolutionarily conserved structure and functions

[48, 59]. CHCHD4 and Mia40 shared the same principal catalytic activity, which is recognition, binding, and oxidative folding through formation of intramolecular disulfide bonds of substrates containing two cysteine-x3-cysteine (twin Cx3C) or two cysteine-x9-cysteine (twin Cx9C) motifs [60]. Thus, the roles of AIF in mitochondrial bioenergetics are linked to the functions of these sets of substrates, for example TIM proteins involved in protein import, CHCHD proteins in cristae integrity, respiratory chain function and regulation of apoptosis, OXPHOS complex subunits in respiratory chain biogenesis, and TRIAP1 in lipid homeostasis [14, 48, 55, 61, 62]. Complete knockout of AIF in HEK293 cells diminished the levels of three subunits of complex I (NDUFA8, NDUFB7, NDUFS5) which are dependent on CHCHD4 for mitochondrial import, contributing to the overall loss of complex I. Among these, NDUFS5 demonstrated a drastically rapid decay and severely impaired interaction with CHCHD4, thus limiting complex I assembly. Moreover, CHCHD4 substrates relevant to complex III and IV also decreased, albeit to a lesser extent and did not induce a delay in assembly or decrease in the expression and activity of these complexes [55]. CHCHD4 was reported to interact with CHCHD3 at C193 and mediate its correct folding and retention in the IMS, contributing to the maintenance of cristae integrity, mitochondrial bioenergetics and cell proliferation [61, 63]. In addition to its role in sustaining mitochondrial morphology, the CHCHD4 substrate TRIAP1 is crucial for intramitochondrial transfer of phospholipids, thus suggesting the relevance of AIF to cristae integrity and lipid homeostasis [62, 64]. Altogether, through mediating the import of CHCHD4 itself and contributing to the CHCHD4-dependent import pathway of nuclear-encoded proteins, AIF is involved in the called anterograde signaling from the nucleus to mitochondria, and thus, could influence different aspects of mitochondrial structure and activities.

AIF mutations and mitochondrial diseases: pathologies, classification, and clinical relevance

Considering the roles of AIF in cell death and mitochondrial metabolism, it is predictable that *AIFM1* mutations could result in human pathologies (Table 1). Indeed, the first cases of early-onset, severe mitochondrial encephalomyopathy induced by *AIFM1* mutation were described

Table 1 List of examples *AIFM1* mutations classified by clinical outcome. COXPD6, combined oxidative phosphorylation deficiency type 6; CMTX4, X-linked Charcot-Marie-Tooth disease type 4

Classification	AIFM1 variants	AIF variants	Clinical phenotypes
COXPD6	**c.506 C > T**	p.Pro169Leu (P169L)	Severe multisystem pathology, metabolic acidosis, mitochondrial dysfunction, and early death [65]
	c.del601-603	Arg201 deletion (R201 del)	Early-onset, severe mitochondrial encephalomyopathy
	c.923G > A	p.Gly308Glu (G308E)	Prenatal ventriculomegaly [66,67]
	c.1013G > A	p.Gly338Glu (G338E)	Severe and early-onset encephalopathy, muscular atrophy and motor axonal neuropathy [66,68]
	c.1436 A > G	p.Gln479Arg (Q479R)	Encephalopathy, mitochondrial disease, metabolic acidosis [69]
CMTX4	**c.422 C > T**	p.Thr141Ile (T141I)	Cerebellar ataxia, hearing loss, neuropathy [70]
	c.470 C > T	p.Ala157Val (A157V)	Severe cerebellar ataxia, neuropathy, atypical hemifacial spasm [71]
	c.513G > A	p.Met171Ile (M171I)	Isolated axonal motor and sensory neuropathy [72]
	c.629T > C	p.Phe210Ser (F210S)	Motor neuropathy [73]
	c.630 C > G	p.Phe210Leu (F210L)	Isolated axonal polyneuropathy [74]
	c.727G > T	p.Val243Leu (V243L)	Progressive muscular atrophy, ataxia and hearing loss [66,75]
	c.784G > A	p.Gly262Ser (G262S)	Axonal neuropathy, hearing loss, cognitive impairment [66,76]
	c.1019T > C	p. Met340Thr (M340T)	Cerebellar ataxia, hearing loss, sensorimotor neuropathy, color blindness, muscle weakness [70,77,78]
	c.1463 C > T	p.Pro488Leu (P488L)	Postlingual progressive hearing loss, distal muscle wasting, unsteady ataxic gait [79]
	c.1478 A > T	p.Glu493Val (E493V)	Slowly progressive axonal neuropathy, deafness, and cognitive impairment [80]
unclassified	**c.705G > C**	p.Gln235His (Q235H)	X-linked hypomyelinating leukodystrophy and spondylometaphyseal dysplasia, mental retardation [81]
	c.720 C > T	p.Asp240Asp (D240D)	
	c.710 A > T	p.Asp237Val (D237V)	
	c.710 A > G	p.Asp237Gly (D237G)	
	c.1195G > A	p.Gly399Ser (G399S)	Childhood-onset nonprogressive cerebellar ataxia, hearing loss, intellectual disability, peripheral neuropathy, mood and behavioral disorder [82]
	c.1357G > C	p.Glu453Gln (E453Q)	Hearing impairment, ataxic sensory neuronopathy [83]
	c.1474T > C	p.Tyr492His (Y492H)	Mitochondrial disorder, combined OXPHOS defect [84]

in 2010 [65]. The modification was reported as a deletion of the arginine residue at position 201 (Arg201 del) in the full-length AIF. In in silico analysis, this residue participates in the β-hairpin (191–203) forming the FAD binding pouch and induces the folding of the regulatory peptide (509–559) regulating the accessibility of the FAD-containing active site. Further investigation on patient samples revealed a reduction in the activity of complex III and complex IV, as well as decreased stability of AIF in both mitochondrial, IMS-bound and soluble forms. Unlike previous in vitro studies of AIF deficiency, no effect on complex I was reported for this *AIFM1* mutation. In addition, soluble Arg201 del AIF showed higher affinity to DNA, which was relevant to the observed increase in parthanatos. It was concluded that deletion of Arg201 mostly affected the functions of the protein, and not its structure.

Since the aforementioned mutant AIF-induced pathological condition, there have been more than 20 cases in literature, with varying clinical manifestations, degrees of severity, and sites of mutation, making their categorization a challenge. One might hypothesize that similar mutational hotspots, such as in the FAD-binding domain, could result in comparable structural and functional perturbations in the protein, as well as clinical outcome in patients. For example, both Met171 and Phe210 are positioned in the first FAD-binding domain of AIF, and patients harboring mutations at these residues (c.513G > A, p.Met171Ile and c.629T > C, p.Phe210Ser) exhibited similar symptoms of motor and sensory neuropathy associated with X-linked Charcot-Marie-Tooth disease type 4 (CMTX4, also known as Cowchock syndrome [72, 73]. As Met171 is close to the regulatory peptide (509–559), Met171Ile was predicted to disrupt the activity of this domain, therefore affecting the susceptibility of AIF to calpain and its interactions with DNA. Phe210Ser was also modelled to disturb the regulatory peptide (509–559), leading to changes in NAD binding capacity. Only the mutation Phe210Ser was evaluated cellularly, showing a decrease in the protein expression level of AIF and fragmentation of the mitochondrial network.

However, the relationship between mutational sites in AIF and structural, functional, as well as clinical consequences is much more ambiguous, possibly due to the complexity of the 3D conformation of the protein. One example is the *AIFM1* variant c.630 C > G, p.Phe210Leu [74]. Even though patients having mutations at residue 210 exhibited the same symptoms of CMTX4, unlike Phe210Ser, Phe210Leu did not affect AIF protein level. More interestingly, western blot analysis of the patient's sample demonstrated lower expression of complex I and III, without any evidence of decreased CHCHD4 protein level or disrupted AIF-CHCHD4 binding, which is necessary for ETC biogenesis. Thus, the authors raised the question of whether the FAD-binding domain has a role in the assembly of the OXPHOS complexes. Another study by Moss et al. on the variant c.506 C > T, p.Pro169Leu further emphasized the complexity of predicting phenotype based on mutational site in AIF [85]. Despite the close position to Met171, this mutation at Pro169 resulted in much more severe clinical outcomes including multisystem pathology, metabolic acidosis, mitochondrial dysfunction, and early death. Functional analysis revealed reduced protein expression levels of AIF and complex I in fibroblasts, as well as complete absence of complex IV in muscle. Therefore, it was suggested that the common feature of the most severe cases is deficiency in complex I and IV. Unfortunately, in silico analysis of Pro169Leu mutant AIF or the consequences of Met171Ile on OXPHOS complexes have not been mentioned, leaving the comparison incomplete. In addition to how mutations at the same site (Phe210Ser, Phe210Leu) and at two close sites (Pro169Leu, Met171Ile) could exhibit different biological and clinical consequences, studies on mutations in the same region of AIF also highlight the puzzling relationship between site of mutations, patient's diagnosis, and protein properties. Similar to residues 169, 171 and 210 discussed above, Val243 is in the first FAD-binding domain of AIF. Despite exhibiting no modifications in the folding, redox, or DNA binding properties, the Val243Leu mutant AIF (c.727G > T) still results in clinical phenotype of progressive muscular atrophy, ataxia, and hearing loss [66, 75]. As only a decrease in the protein level of AIF was reported, and computer modelling demonstrated unlikely interaction of this residue to partners such as CHCHD4, it was hypothesized that the observed pathology resulted from reduced AIF expression.

Similar to the FAD-binding domain, the NADH-binding domain is also a hotspot for AIF mutations. One of the most characterized and clinically severe mutations in this region is p.Gly308Glu (c.923G-NA), resulting in prenatal ventriculomegaly [67]. Gly308 is involved in the NADH-binding channel and also orientates Leu342 and Gly336 for AIF-NAD + complex stability. Therefore, the Gly308Glu AIF variant exhibited decreased affinity for NADH, as well as insufficient formation of CTC [66]. In addition, inefficient electron transfer from NADH to AIF was hypothesized to affect the binding of AIF to its partner CHCHD4, which could explain the reduction in muscle complex I activity and OXPHOS-related encephalopathy and muscle atrophy in the patient. On the contrary, another mutation in the NADH-binding domain, p.Gly338Glu (c.1013G > A), did not show a strong correlation between genotype and phenotype. Patients harboring this mutation exhibited severe and early-onset encephalopathy, muscular atrophy and motor axonal neuropathy. Nonetheless, no significant change in the

binding to NADH and only moderate effect on redox properties were reported for this AIF variant. In addition, no serious defects in the OXPHOS system were found, except for a decline in the activity of complex IV. Similar to Val243Leu, it was suggested that the clinical outcome of Gly338Glu might be triggered by decreased AIF protein expression. In addition to mutations of residues positioned in the FAD- or NADH-binding domains, AIF variants in other regions such as the C-terminal also induce pathological conditions. One example would be p.Glu493Val (c.1478 A > T), causing CMTX4 with slowly progressive axonal neuropathy, deafness and cognitive impairment [80]. This AIF variant exhibited unstable conformation, lower binding affinity for NADH and higher affinity for DNA. Further study revealed increases in DNA fragmentation, parthanatos and nuclear translocation of AIF, despite no impairment in the respiratory chain complexes or fragmentation of the mitochondrial network.

As evident by all variants described above, with the inconsistent genotype-phenotype correlation, a precise molecular or cellular classification of AIF mutations has yet to be established. So far, a classification based on clinical outcome of the patients, consisting of combined oxidative phosphorylation deficiency type 6 (COXPD6), CMTX4, and X-linked neuropathy-associated deafness has been established [86]. Accordingly, Arg201del, Gly308Glu, Gly338Glu, and Pro169Leu can be grouped together with the patients exhibiting severe, neonatal encephalomyopathy. Other mutations previously mentioned (Met171Ile, Phe210Ser, Phe210Leu, Val243Leu, Glu493Val) would be examples of CMTX4, highlighted by later-onset axonal neuropathy, hearing loss and cognitive impairment. For the group of X-linked deafness associated with neuropathy, the mutation p.Leu344Phe (c.1030 C > T) has been reported to be the most common [87]. In addition, novel AIF variants were identified in a group of 12 patients with X-linked progressive skeletal and neurologic disorders [81] which has expanded the spectrum of clinical outcome. Several uncategorized cases with varied phenotypes have also been reported, emphasizing the heterogeneous nature of mutant AIF-induced pathologies (table 1). Considering the growing number of clinically relevant AIF mutations, more research is required to understand them in a systemic way and to develop better classification. AIF variants should be studied on biophysical, biochemical and cellular levels, including all changes in protein structure, folding, stability, binding to FAD, NADH and DNA, interactions with partners such as CHCHD4, as well as effects on OXPHOS complexes and cell death.

Targeting AIF: a promising avenue for cancer therapy

In addition to human pathologies related to the nervous, muscular and auditory systems, there is emerging evidence suggesting the potential involvement of AIF in cancer. Mutational analysis using single-strand conformation polymorphism (SSCP) of exons 10–15 encoding the region involved in cell death function of AIF has been done in samples of colorectal, gastric, breast and liver cancers, as well as leukemias [88]. Only one two-base deletion in intron 15 was found in colorectal carcinomas, suggesting that mutations in AIF are rare in common cancers. Due to limited literature on the subject and considering that AIF also has a role in mitochondrial bioenergetics, we could not exclude the possibility of mutations in other regions of the protein. On the other hand, most studies have focused on changes in the expression levels of AIF in cancer, usually upregulation. Elevated mRNA and/or protein expression levels of AIF have been implied in studies on lung adenocarcinoma and different lung cancer subtypes, pancreatic cancer, prostate cancer, colorectal carcinomas, gastric carcinomas, esophageal squamous cell carcinoma, and skin squamous cell carcinoma [88–94]. For breast cancer, *AIFM1* was reported as a high-risk prognostic marker and part of an apoptosis-related gene signature [95].

The consequences of AIF deficiency have been explored in different cancer types, both in vitro and in vivo. For example, mouse models of *AIFM1*-knocked-out *Kras*-mutated non-small-cell lung carcinomas (NSCLCs) showed prolonged overall survival, decreased tumor burden and reduced progression into adenocarcinomas compared to WT controls [92]. The collected primary pneumocytes demonstrated impaired mitochondrial structure, lower expression levels for proteins of OXPHOS complex I (NDUFB6, NDUFS3) and defective mitochondrial respiration, evident by decreases in basal oxygen consumption rate (OCR), ATP-linked respiration and maximal respiratory capacity. Likely relevant to the reported OXPHOS deficiency, AIF deletion also induced a switch to glycolysis for energetic metabolism in these primary pneumocytes. *Kras*-mutant human NSCLC A549 cells with stable knockdown of AIF by shRNA exhibited reduced expression levels of subunits in OXPHOS complexes I (NDUFB8), III (UQCRC2) and IV (COXII) as well as AIF's partner CHCHD4, which was relevant to impaired mitochondrial respiration. Moreover, AIF depletion was found to negatively affect the proliferation and clonogenic potential in a panel of human lung cancer cell lines with either wildtype or mutant *Kras*. In another study, analysis of five different pancreatic cancer cell lines revealed a link between AIF and metabolic plasticity [93]. These cells were evaluated for basal metabolic phenotypes then subjected to

AIF ablation by shRNA. Decreased proliferation and migration were only reported in AIF-deficient cell lines with moderate to high reliance on OXPHOS, correlating with decreased expression of complex I subunits. AIF deficiency also increased glucose consumption and resensitized two of these cell lines to the glycolysis inhibitor 2-DG. These findings suggested that AIF could be involved in metabolic plasticity through regulating the balance between glycolysis and OXPHOS. In addition to lung and pancreatic cancer, AIF was demonstrated to support the survival and progression of advanced prostate cancer [91]. AIF-deficient aggressive prostate cancer cell lines showed significantly decreased proliferation and signs of cell death in growth stress conditions, impaired in vitro invasion capacity, as well as lower tumorigenesis after subcutaneous injection in athymic nude mice. Reduction in the protein expression levels complex I subunits was reported for both cell lines and xenografts. Metabolically, *AIFM1* ablation resulted in lower oxygen consumption, higher glucose dependency and increased lactate secretion, implicating a switch from OXPHOS to glycolysis. Interestingly, introduction of AIF carrying mutations at two residues involved in NADH-oxidase activity (Thr263Ala/Val300Ala) in these cells restored the expression of complex I subunits without reverting the increased glucose consumption or impaired growth. Therefore, the authors argued that the enzymatic activity of AIF was necessary for aggressiveness of prostate cancer. To summarize, it could be noted that for cancer types with elevated AIF expression, induced deficiency usually decreased the levels of complex I subunits, impaired mitochondrial respiration, and switched the cells to glycolysis for energetic needs. This highlights the importance of AIF in sustaining functional respiratory chain and OXPHOS, supporting proliferation, and promoting progression in these cancers. As AIF has been shown to interact with CHCHD4 and participate in the AIF/CHCHD4 import machinery for several protein substrates of the OXPHOS complexes, it is possible to hypothesize about interruption of this binding as a treatment approach.

Considering the dual functions of AIF, it is not surprising to find the reverse scenario, where AIF protein expression level decreases compared to healthy control, such as reported in renal cell carcinoma (RCC) [38]. No significant *AIFM1* mutations were found, and the downregulation likely resulted from aberrant methylation of the *AIFM1* promoter. RCC cell lines transiently overexpressing AIF showed increased apoptosis, AIF translocation into the nuclei and more activation of AIF's partner Serine/threonine-protein kinase 3 (STK3) involved in apoptosis, without changes in caspase 3 activity. These findings suggest that AIF overexpression in RCC cells could induce AIF-mediated caspase-independent apoptosis, and WT cells might have developed mechanisms to lower AIF expression and avoid cell death. In addition, as different organs showed varying AIF basal expression levels [38] the activity of AIF is potentially tissue specific. Thus, there is likely a maintenance of balance between the anti-apoptotic and pro-apoptotic roles of AIF in cancers, and evaluation of AIF expression levels in patient samples is crucial before considering treatment targeting AIF.

To illustrate this argument and further investigate the relevance of AIF in cancer, analysis of patient survival by *AIFM1* expression level in public databases was conducted on the R2 Genomics Analysis and Visualization Platform (https://hgserver1.amc.nl/cgi-bin/r2/main.cgi). Cox regression analysis was used to evaluate the relationship between *AIFM1* expression and decreased or increased survival, with the output as Cox proportional hazard. Values greater than 1 indicate that higher expression level is associated with poor prognosis (Table 2), and values smaller than 1 suggest the opposite (Table 3). High *AIFM1* levels generally correlate with decreased survival in various cancer types such as neuroblastoma, prostate adenocarcinoma, melanoma, lung adenocarcinoma, breast cancer, chromophobe renal cell carcinoma, esophageal carcinoma, lymphoma and myeloma ($p < 0.05$). Therefore, it is reasonable to anticipate more studies on the exact mechanisms of AIF in specific cancers, and the exploitation of this highly potential, yet underappreciated target for the development of novel anti-cancer drugs. As previously mentioned, one such scenario would be to inhibit AIF/CHCHD4 interaction and thus diminish the pro-survival roles of AIF in mitochondrial bioenergetics.

Conclusion

Since its discovery over two decades ago, our understanding of AIF has expanded significantly. This review provides general knowledge of AIF in terms of its structure, life and death functions, and implications in diseases, particularly mutated *AIFM1*-induced pathologies and the potential of targeting AIF in cancer. Structurally, AIF possesses distinct domains that regulate its import, processing, redox activity, as well as interactions with partners. Thus, there exists a structure-function relationship that determines the dual roles of AIF in cell death and survival, in response to cellular physiological conditions. Beyond its function in caspase-independent cell death (parthanatos), AIF mediates different mitochondrial activities such as OXPHOS, lipid homeostasis and maintenance of cristae integrity through contributing to the CHCHD4 import pathway. Thus, dysregulation of the protein has been implied in various pathological conditions, from neuromuscular and metabolic disorders to cancer.

Table 2 Correlation between high AIFM1 expression and poorer survival. Analysis of patient survival by *AIFM1* expression levels on R2 Genomics Analysis and Visualization Platform using available public datasets. Overall survival and/or progression-free survival were performed to estimate survival curves using Kaplan-Meier method. Survival cut-off was automatically determined in a scanning approach, in which every increasing value was used to create two groups, *p*-value was tested using a log-rank test, and the most significant expression cut-off was reported. *p*-value < 0.05 (5.0E-02) was considered statistically significant. Cox proportional hazard above 1 associates high *AIFM1* expression with decreased survival in patients

Cancer type	Dataset	Survival type	*p*-value
Tumor neuroblastoma	Cangelosi 786 - overall [96]	overall	1.00E-24
Tumor neuroblastoma	Cangelosi 786 - eventfree [96]	event free	5.20E-21
Tumor neuroblastoma	SEQC 498 - eventfree - GSE62564 [97]	event free	1.10E-17
Tumor neuroblastoma	SEQC 498 - overall - GSE62564 [97]	overall	2.60E-17
Tumor neuroblastoma	Kocak 649 - eventfree - GSE45547 [98]	event free	1.40E-15
Tumor neuroblastoma	Oberthuer 251 - eventfree - E-TABM-38 [99]	event free	2.30E-11
Tumor neuroblastoma	Oberthuer 251 - overall - E-TABM-38 [99]	overall	1.70E-08
Tumor neuroblastoma	SEQC 498 - eventfree - GSE49710 [97]	event free	4.50E-07
Tumor neuroblastoma	SEQC 498 - overall - GSE49710 [97]	overall	4.7E-06
Tumor neuroblastoma	NRC 283 - overall - GSE85047 [100]	overall	1.7E-05
Tumor neuroblastoma	NRC 283 - progressionfree - GSE85047 [100]	progression free	7.8E-05
Tumor neuroblastoma	Versteeg 122 - progrfree-1304 [101]	progression free	1.2E-04
Tumor neuroblastoma	Kocak 649 - overall - GSE45547 [98]	overall	2.00E-04
Tumor neuroblastoma	Maris 101 - progressionfree - GSE3960 [102]	progression free	4.4E-04
Tumor neuroblastoma	Maris 101 - overall - GSE3960 [102]	overall	8.4E-04
Tumor neuroblastoma	Versteeg 122 - overall-1304 [101]	overall	1.4E-03
Tumor neuroblastoma	Versteeg 88 - overall-c1103 - GSE16476 [101]	overall	1.5E-03
Tumor neuroblastoma	Versteeg 122 - overall-1302 [101]	overall	2.1E-03
Tumor neuroblastoma	Westermann 144 - overall [103]	overall	2.2E-03
Mixed prostate adenocarcinoma	tcga 553 - overall [104]	overall	2.5E-03
Tumor melanoma metastatic	Bhardwaj 44 - overall - GSE19234 [105]	overall	2.9E-03
Tumor lung adenocarcinomas	Kohno 246 - relapsefree - GSE31210 [106,107]	relapse free	3.0E-03
Tumor breast	Bergh 159 - overall - GSE1456 [108]	overall	3.2E-03
Tumor skin cutaneous melanoma	tcga 473 - overall [109]	overall	3.5E-03
Tumor neuroblastoma	Westermann 144 - eventfree [103]	event free	4.2E-03
Mixed kidney chromophobe	tcga 90 - overall [110]	overall	4.4E-03
Tumor B-cell lymphoma	Xiao 420 - overall - GSE10846 [111]	overall	5.2E-03
Tumor neuroblastoma	Versteeg 88 - relapsefree-c1103 - GSE16476 [101]	relapse free	5.4E-03
Tumor esophageal carcinoma	TCGA 184 - overall - ESCA [112]	overall	6.8E-03
Tumor breast	Bergh 159 - relapsefree - GSE1456 [108]	relapse free	8.0E-03
Tumor mantle cell lymphoma	Staudt 122 - overall - GSE93291__1 [113]	overall	1.5E-02
Tumor myeloma	Hanamura 542 - overall - GSE2658 [114]	overall	1.9E-02
Tumor skin cutaneous melanoma	TCGA 375 - overall - SKCM [109]	overall	3.0E-02
Tumor neuroblastoma non MYCN amplified	Seeger 102 - relapsefree - GSE3446 [115]	relapse free	3.6E-02
Tumor lung	Bild 114 - overall - GSE3141 [116]	overall	7.2E-02
Tumor Wilms	OCG 125 - overall [117]	overall	7.7E-02
Tumor Ewing sarcoma	Dirksen 85 - eventfree - GSE63157__1 [118]	event free	7.9E-02
Tumor lung adenocarcinomas	Kohno 246 - overall - GSE31210 [106,107]	overall	7.9E-02
Tumor Ewing sarcoma	Dirksen 85 - overall - GSE63157__1 [118]	overall	1.2E-01
Tumor melanoma	Jönsson 214 - distantmetastasis_free - GSE65904 [119]	distant metastasis free	1.2E-01
Tumor uveal melanoma	tcga 80 - overall [120]	overall	1.5E-01
Tumor medulloblastoma	Williamson 331 - overall - emtab10767 [121]	overall	1.7E-01
Tumor medulloblastoma	Cavalli 763 - overall - GSE85217 [122]	overall	1.8E-01
Tumor glioma pediatric	Paugh 53 - overall - GSE19578 [123]	overall	2.2E-01
Tumor T-cell lymphoma	Wang 62 - progessionfree - GSE168508 [124–126]	progression free	2.3E-01
Tumor neuroblastoma	Asgharzadeh 249 - overall [127]	overall	2.3E-01
Tumor uterine carcinoma	tcga 57 - overall [128]	overall	2.4E-01
Tumor T-cell lymphoma	Wang 62 - overall - GSE168508 [124–126]	overall	2.4E-01
Tumor hodgkin lymphoma	Steidl 34 - overall - GSE39133 [129]	overall	2.6E-01

Table 2 (continued)

Cancer type	Dataset	Survival type	*p*-value
Tumor lymphoma (T-cell peripheral)	Rosenwald 193 - overall - GSE58445 [130]	overall	3.0E-01
Tumor thymona	TCGA 120 - overall - THYM [131]	overall	3.4E-01
Tumor lymphoid neoplasm diffuse large B-cell lympho	tcga 48 - overall [132]	overall	3.5E-01
Tumor oral	Mao 86 - cancerfree - GSE26549 [133]	cancer free	4.9E-01
Tumor neuroblastoma	Asgharzadeh 249 - eventfree [127]	event free	4.9E-01

Table 3 Correlation between high AIFM1 expression and better survival. Analysis of patient survival by *AIFM1* expression levels on R2 Genomics Analysis and Visualization Platform using available public datasets. Overall survival and/or progression-free survival were performed to estimate survival curves using Kaplan-Meier method. Survival cut-off was automatically determined in a scanning approach, in which every increasing value was used to create two groups, *p*-value was tested using a log-rank test, and the most significant expression cut-off was reported. *p*-value < 0.05 (5.0E-02) was considered statistically significant. Cox proportional hazard below 1 suggests high *AIFM1* expression as better prognosis

Cancer type	Dataset	Survival type	*p*-value
Tumor adrenocortical carcinoma	TCGA 79 - overall - ACC [134]	overall	1.3E-06
Tumor colon	Nunes 1063 - recurrencefree [135]	recurrence free	2.7E-05
Mixed kidney renal clear cell carcinoma	tcga 609 - overall [136]	overall	1.5E-04
Tumor colon	Nunes 1063 - overall [135]	overall	3.3E-04
Tumor kidney renal papillary cell carcinoma	TCGA 290 - overall - KIRP [137]	overall	2.2E-03
Tumor glioblastoma	TCGA 540 - progrfree [138]	progression free	5.8E-03
Mixed gastric	Nebozhyn 400 - recurrence - GSE66229 [139]	recurrence	6.8E-03
Tumor colon	Guinney 3232 - overall - syn2623706 [140]	overall	7.9E-03
Tumor pancreatic ductal adenocarcinoma	Yeh 132 - overall - GSE21501 [141]	overall	9.5E-03
Tumor pancreatic	Bailey 96 - overall [142]	overall	2.8E-02
Mixed gastric	Nebozhyn 400 - overall - GSE66229 [139]	overall	3.8E-02
Tumor ovarian adenocarcinoma (oxidative stress)	Mechta-Grigoriou 107 - overall - GSE26193 [143]	overall	4.3E-02
Tumor ovarian adenocarcinoma (oxidative stress)	Mechta-Grigoriou 107 - pfs - GSE26193 [143]	progression free	9.3E-02
Tumor pancreatic adenocarcinoma	TCGA 178 - overall - PAAD [144]	overall	1.1E-01
Tumor mesothelioma	tcga 87 - overall [145]	overall	1.2E-01
Tumor ovarian	Pamuła-Piłat 101 - evenfree - GSE63885 [146]	event free	2.0E-01
Tumor ovarian	Pamuła-Piłat 101 - overall - GSE63885 [146]	overall	3.3E-01
Tumor neuroblastoma	Bell 97 - overall - GSE181582 [147]	overall	3.9E-01
Tumor ovarian serous cystadenocarcinoma	tcga 381 - overall [148]	overall	5.3E-01
Tumor neuroblastoma	Bell 97 - progressionfree - GSE181582 [147]	progression free	5.5E-01
Tumor rectal (multimodal therapy)	Ghadimi 245 - overall - GSE40492 [149]	overall	5.8E-01
Tumor pancreatic ductal adenocarcinoma	linkedomics 140 - overall [150]	overall	5.9E-01
Tumor hodgkin lymphoma	Steidl 34 - progressionfree - GSE39133 [129]	progression free	7.8E-01
Tumor Wilms	OCG 148 - overall [117]	overall	8.4E-01
Tumor rhabdomyosarcomas	Tran 158 - overall - GSE167059 [151]	overall	9.2E-01

Mutations in the *AIFM1* gene lead to a spectrum of pathologies that have been mainly classified according to clinical outcomes, including Combined OXPHOS Deficiency Type 6 (COXPD6), Charcot-Marie-Tooth Disease Type 4 (CMTX4), and X-linked neuropathies with hearing loss. Although certain mutations have shown a strong correlation between genotype and phenotype, there exist AIF variants which show less severe changes than predicted from clinical symptoms. This emphasizes the complex structure-function relationship of AIF in the pathogenesis of these mitochondrial diseases. Meanwhile, in cancer, AIF exhibits both tumour-promoting and tumour-suppressing characteristics. In cancer with AIF upregulation, the protein supports proliferation and disease progression through sustaining OXPHOS activity. On the contrary, decreased expression enables some cancers to evade AIF-dependent cell death.

Several compounds that trigger parthanatos have shown efficacy against different types of cancer, yet the upstream and downstream consequences remain to be further elucidated. Moreover, as described above, there is likely a balance between the pro-death and pro-survival roles of AIF in cancer. This highlights the need to examine the expression levels as well as functions of AIF specific to each cancer type before considering AIF-targeted therapies. To abolish AIF's pro-survival roles that benefit cancer progression, it is possible to develop molecules

that disrupt its interaction with CHCHD4, potentially providing a novel approach for anticancer therapy.

Finally, in a translational perspective, future research should focus on the interactome of AIF in both cell death and cell survival, AIF in disease initiation and progression, and therapeutic strategies exploiting its involvement in mitochondrial disorders and in cancer.

Abbreviations

AIF	Apoptosis-inducing factor
CHCHD4	Coiled-coil-helix-coiled-coil-helix domain containing 4
CMTX4	X-linked Charcot-Marie-Tooth disease type 4
COXPD6	Combined oxidative phosphorylation deficiency type 6
CTC	Charge-transfer-complex
CypA	Cyclophilin A
Cyt c	Cytochrome c
EndoG	Endonuclease G
ER	Endoplasmic reticulum
ESCs	Embryonic stem cells
ETC	Electron transport chain
FAD	Flavin adenine dinucleotide
Hq mice	Harlequin mice
Hsp70	Heat shock protein 70
IMM	Inner mitochondrial membrane
IMS	Intermembrane space
JNK	c-Jun N-terminal protein kinases
KO	Knock-out
MIF	Macrophage migration inhibitory factor
MLS	Mitochondrial localization sequence
MNNG	N-methyl-N′-nitro-N-nitrosoguanidine
MPP	Mitochondrial processing peptidase
NADH/NADPH	Reduced nicotinamide adenine dinucleotide/reduced nicotinamide adenine dinucleotide phosphate
NMDA	N-methyl-D-aspartate
NSCLCs	Non-small-cell lung carcinomas
OCR	Oxygen consumption rate
OMM	Outer mitochondrial membrane
OSCC	Oral squamous cell carcinoma
OTUD1	OTU deubiquitinase 1
OXPHOS	Oxidative phosphorylation
PAK5	p21 activated kinase 5
PAR	Poly(ADP-ribose)
PARP	Poly(ADP-ribose) polymerase
PBM	PAR-binding motif
PCD	Programmed cell death
RCC	Renal cell carcinoma
ROS	Reactive oxygen species
SSCP	Single-strand conformation polymorphism
STK3	Serine/threonine-protein kinase 3
XIAP	X-linked inhibitor of apoptosis

Acknowledgements
Figures were created with BioRender.com.

Author contributions
TNA.N., HT.L. and C.B. wrote the main manuscript text and TNA.N prepared figures and tables. All authors reviewed the manuscript.

Funding
CB research was supported by grants from the French National Cancer Institute "INCa 2017-1-PL BIO-08" and "2021 – 167/ INCA_16344" and the Société française de lutte contre les cancers et les leucémies de l'enfant et de l'adolescent (SFCE), grant number ECS 20, PHC PESSOA, N°49163TL and the Groupement des Entreprises Francaises dans la lutte contre le Cancer [2023–2024].

Data availability
No datasets were generated or analysed during the current study.

Declarations

Competing interests
The authors declare no competing interests.

Received: 17 March 2025 / Accepted: 27 May 2025
Published online: 04 June 2025

References

1. Javadov S, Kozlov AV, Camara AK. S. Mitochondria in health and diseases. Cells. 2020;9:1177.
2. Nunnari J, Suomalainen A. Mitochondria: in sickness and in health. Cell. 2012;148:1145–59.
3. Kotrys AV, Szczesny RJ. Mitochondrial gene expression and Beyond—Novel aspects of cellular physiology. Cells. 2019;9:17.
4. Gorman GS, et al. Mitochondrial diseases. Nat Rev Dis Primers. 2016;2:1–22.
5. Vitale I, et al. Apoptotic cell death in disease-Current Understanding of the NCCD 2023. Cell Death Differ. 2023;30:1097–154.
6. Souers AJ, et al. ABT-199, a potent and selective BCL-2 inhibitor, achieves antitumor activity while sparing platelets. Nat Med. 2013;19:202–8.
7. Kroemer G, Galluzzi L, Brenner C. Mitochondrial membrane permeabilization in cell death. Physiol Rev. 2007;87:99–163.
8. Wang C, Youle RJ. The role of mitochondria in apoptosis. Annu Rev Genet. 2009;43:95–118.
9. Fatokun AA, Dawson VL, Dawson TM. Parthanatos: mitochondrial-linked mechanisms and therapeutic opportunities. Br J Pharmacol. 2014;171:2000–16.
10. Susin SA, et al. Molecular characterization of mitochondrial apoptosis-inducing factor. Nature. 1999;397:441–6.
11. Otera H, Ohsakaya S, Nagaura Z-I, Ishihara N, Mihara K. Export of mitochondrial AIF in response to proapoptotic stimuli depends on processing at the intermembrane space. EMBO J. 2005;24:1375–86.
12. Pacher P, Szabo C. Role of the Peroxynitrite-Poly(ADP-Ribose) polymerase pathway in human disease. Am J Pathol. 2008;173:2–13.
13. Wang Y, et al. A nuclease that mediates cell death induced by DNA damage and poly(ADP-ribose) polymerase-1. Science. 2016;354:aad6872.
14. Hangen E, et al. Interaction between AIF and CHCHD4 regulates respiratory chain biogenesis. Mol Cell. 2015;58:1001–14.
15. Maté MJ, et al. The crystal structure of the mouse apoptosis-inducing factor AIF. Nat Struct Biol. 2002;9:442–6.
16. Ye H, et al. DNA binding is required for the apoptogenic action of apoptosis inducing factor. Nat Struct Biol. 2002;9:680–4.
17. Churbanova IY, Sevrioukova IF. Redox-dependent changes in molecular properties of mitochondrial apoptosis-inducing factor. J Biol Chem. 2008;283:5622–31.
18. Sevrioukova IF. Redox-linked conformational dynamics in apoptosis inducing factor. J Mol Biol. 2009;390:924–38.
19. Wilkinson JC, Wilkinson AS, Galbán S, Csomos RA, Duckett CS. Apoptosis-Inducing factor is a target for ubiquitination through interaction with XIAP. Mol Cell Biol. 2008;28:237–47.
20. Lewis EM, Wilkinson AS, Davis NY, Horita DA, Wilkinson JC. Nondegradative ubiquitination of apoptosis inducing factor (AIF) by X-Linked inhibitor of apoptosis at a residue critical for AIF-Mediated chromatin degradation. Biochemistry. 2011;50:11084–96.
21. Luo Q, et al. OTUD1 activates Caspase-Independent and Caspase-Dependent apoptosis by promoting AIF nuclear translocation and MCL1 degradation. Adv Sci (Weinh). 2021;8:2002874.
22. Xing Y, et al. PAK5-mediated AIF phosphorylation inhibits its nuclear translocation and promotes breast cancer tumorigenesis. Int J Biol Sci. 2021;17:1315–27.
23. Polster BM, Basañez G, Etxebarria A, Hardwick JM, Nicholls DG. Calpain I induces cleavage and release of apoptosis-inducing factor from isolated mitochondria. J Biol Chem. 2005;280:6447–54.
24. Cao G, et al. Critical role of Calpain I in mitochondrial release of Apoptosis-Inducing factor in ischemic neuronal injury. J Neurosci. 2007;27:9278–93.
25. Ravagnan L, et al. Heat-shock protein 70 antagonizes apoptosis-inducing factor. Nat Cell Biol. 2001;3:839–43.
26. Candé C, et al. AIF and Cyclophilin A cooperate in apoptosis-associated chromatinolysis. Oncogene. 2004;23:1514–21.

27. Zhu C, et al. Cyclophilin A participates in the nuclear translocation of apoptosis-inducing factor in neurons after cerebral hypoxia-ischemia. J Exp Med. 2007;204:1741–8.
28. Bras M, Queenan B, Susin SA. Programmed cell death via mitochondria: different modes of dying. Biochem (Mosc). 2005;70:231–9.
29. Bano D, et al. Alteration of the nuclear pore complex in Ca2+-mediated cell death. Cell Death Differ. 2010;17:119–33.
30. Wang X, Yang C, Chai J, Shi Y, Xue D. Mechanisms of AIF-mediated apoptotic DNA degradation in Caenorhabditis elegans. Science. 2002;298:1587–92.
31. Yu S-W, et al. Mediation of poly(ADP-ribose) polymerase-1-dependent cell death by apoptosis-inducing factor. Science. 2002;297:259–63.
32. Wang Y, Dawson VL, Dawson TM. Poly(ADP-ribose) signals to mitochondrial AIF: A key event in parthanatos. Exp Neurol. 2009;218:193–202.
33. Wang Y, et al. Poly(ADP-ribose) (PAR) binding to apoptosis-inducing factor is critical for PAR polymerase-1-dependent cell death (parthanatos). Sci Signal. 2011;4:ra20.
34. Joza N, et al. Essential role of the mitochondrial apoptosis-inducing factor in programmed cell death. Nature. 2001;410:549–54.
35. Klein JA, et al. The harlequin mouse mutation downregulates apoptosis-inducing factor. Nature. 2002;419:367–74.
36. Cheung ECC, et al. Apoptosis-Inducing factor is a key factor in neuronal cell death propagated by BAX-Dependent and BAX-Independent mechanisms. J Neurosci. 2005;25:1324–34.
37. Tóth-Zsámboki E, et al. Activation of Poly(ADP-Ribose) polymerase by myocardial ischemia and coronary reperfusion in human Circulating leukocytes. Mol Med. 2006;12:221–8.
38. Xu S, et al. AIF downregulation and its interaction with STK3 in renal cell carcinoma. PLoS ONE. 2014;9:e100824.
39. Zhu C, et al. Apoptosis-inducing factor is a major contributor to neuronal loss induced by neonatal cerebral hypoxia-ischemia. Cell Death Differ. 2007;14:775–84.
40. Li D, et al. Oxaliplatin induces the PARP1-mediated parthanatos in oral squamous cell carcinoma by increasing production of ROS. Aging. 2021;13:4242–57.
41. Zhao N, et al. YM155, a survivin suppressant, triggers PARP-dependent cell death (parthanatos) and inhibits esophageal squamous-cell carcinoma xenografts in mice. Oncotarget. 2015;6:18445–59.
42. Leon LJ, Pasupuleti N, Gorin F, Iii KLC. A Cell-Permeant Amiloride derivative induces Caspase-Independent, AIF-Mediated programmed necrotic death of breast Cancer cells. PLoS ONE. 2013;8:e63038.
43. Hojka-Osinska A, Ziolo E, Rapak A. Combined treatment with Fenretinide and indomethacin induces AIF-mediated, non-classical cell death in human acute T-cell leukemia Jurkat cells. Biochem Biophys Res Commun. 2012;419:590–5.
44. Zhou H, et al. Matrine induces caspase-independent program cell death in hepatocellular carcinoma through bid-mediated nuclear translocation of apoptosis inducing factor. Mol Cancer. 2014;13:59.
45. Atiprimod inhibits the. Growth of mantle cell lymphoma in vitro and in vivo and induces apoptosis via activating the mitochondrial pathways. Blood. 2007;109:5455–62.
46. Ma D, et al. Deoxypodophyllotoxin triggers parthanatos in glioma cells via induction of excessive ROS. Cancer Lett. 2016;371:194–204.
47. Jeong JC, et al. Silibinin induces apoptosis via calpain-dependent AIF nuclear translocation in U87MG human glioma cell death. Journal Experimental Clinical Cancer Research: CR. 2011;30:44.
48. Reinhardt C, et al. AIF Meets the CHCHD4/Mia40-dependent mitochondrial import pathway. Biochim Biophys Acta Mol Basis Dis. 2020;1866:165746.
49. Guha M, Avadhani NG. Mitochondrial retrograde signaling at the crossroads of tumor bioenergetics, genetics and epigenetics. Mitochondrion. 2013;13:577–91.
50. Armand A-S, et al. Apoptosis-Inducing factor regulates skeletal muscle progenitor cell number and muscle phenotype. PLoS ONE. 2011;6:e27283.
51. Banerjee H, et al. A role for apoptosis-inducing factor in T cell development. J Exp Med. 2012;209:1641–53.
52. Vahsen N, et al. AIF deficiency compromises oxidative phosphorylation. EMBO J. 2004;23:4679–89.
53. El Ghouzzi V, et al. Apoptosis-inducing factor deficiency induces early mitochondrial degeneration in brain followed by progressive multifocal neuropathology. J Neuropathol Exp Neurol. 2007;66:838–47.
54. Bénit P, Goncalves S, Dassa EP, Brière J-J, Rustin P. The variability of the harlequin mouse phenotype resembles that of human mitochondrial-complex I-deficiency syndromes. PLoS ONE. 2008;3:e3208.
55. Salscheider SL, et al. AIFM1 is a component of the mitochondrial disulfide relay that drives complex I assembly through efficient import of NDUFS5. EMBO J. 2022;41:e110784.
56. Murschall LM, et al. The C-terminal region of the oxidoreductase MIA40 stabilizes its cytosolic precursor during mitochondrial import. BMC Biol. 2020;18:96.
57. Brosey CA, Shen R, Tainer JA. NADH-bound AIF activates the mitochondrial CHCHD4/MIA40 chaperone by a substrate-mimicry mechanism. EMBO J. 2025;1–29. https://doi.org/10.1038/s44318-024-00360-6
58. Pei J, Zhang J, Cong Q. Human mitochondrial protein complexes revealed by large-scale Coevolution analysis and deep learning-based structure modeling. Bioinformatics. 2022;38:4301–11.
59. Hofmann S, et al. Functional and mutational characterization of human MIA40 acting during import into the mitochondrial intermembrane space. J Mol Biol. 2005;353:517–28.
60. Longen S, et al. Systematic analysis of the twin cx(9)c protein family. J Mol Biol. 2009;393:356–68.
61. Darshi M, Trinh KN, Murphy AN, Taylor SS. Targeting and import mechanism of Coiled-coil Helix Coiled-coil Helix Domain-containing protein 3 (ChChd3) into the mitochondrial intermembrane space. J Biol Chem. 2012;287:39480–91.
62. Nedara K, et al. Relevance of the TRIAP1/p53 axis in colon cancer cell proliferation and adaptation to glutamine deprivation. Front Oncol. 2022;12:958155.
63. Darshi M, et al. ChChd3, an inner mitochondrial membrane protein, is essential for maintaining Crista integrity and mitochondrial function. J Biol Chem. 2011;286:2918–32.
64. Pujols J et al. MIA40 circumvents the folding constraints imposed by TRIAP1 function. J Biol Chem 0, (2025).
65. Ghezzi D, et al. Severe X-Linked mitochondrial encephalomyopathy associated with a mutation in Apoptosis-Inducing factor. Am J Hum Genet. 2010;86:639–49.
66. Sevrioukova IF. Structure/Function relations in AIFM1 variants associated with neurodegenerative disorders. J Mol Biol. 2016;428:3650–65.
67. Berger I, et al. Early prenatal ventriculomegaly due to an AIFM1 mutation identified by linkage analysis and whole exome sequencing. Mol Genet Metab. 2011;104:517–20.
68. Diodato D, et al. A novel AIFM1 mutation expands the phenotype to an infantile motor neuron disease. Eur J Hum Genet. 2016;24:463–6.
69. Morton SU, et al. AIFM1 mutation presenting with fatal encephalomyopathy and mitochondrial disease in an infant. Cold Spring Harb Mol Case Stud. 2017;3:a001560.
70. Heimer G, et al. Mutations in AIFM1 cause an X-linked childhood cerebellar ataxia partially responsive to riboflavin. Eur J Paediatr Neurol. 2018;22:93–101.
71. Depierreux F, Alkan S. Atypical hemifacial spasm and myoclonus related to AIFM1 variant. Neuropediatrics. 2022;53:217.
72. Wang B, et al. A novel AIFM1 mutation in a Chinese family with X-linked Charcot-Marie-Tooth disease type 4. Neuromuscul Disord. 2018;28:652–9.
73. Sancho P, et al. A newly distal hereditary motor neuropathy caused by a rare AIFM1 mutation. Neurogenetics. 2017;18:245–50.
74. Hu B, et al. A novel missense mutation in AIFM1 results in axonal polyneuropathy and misassembly of OXPHOS complexes. Eur J Neurol. 2017;24:1499–506.
75. Kettwig M, et al. From ventriculomegaly to severe muscular atrophy: expansion of the clinical spectrum related to mutations in AIFM1. Mitochondrion. 2015;21:12–8.
76. Ardissone A, et al. A slowly progressive mitochondrial encephalomyopathy widens the spectrum of AIFM1 disorders. Neurology. 2015;84:2193–5.
77. Bogdanova-Mihaylova P, et al. Clinical spectrum of AIFM1-associated disease in an Irish family, from mild neuropathy to severe cerebellar ataxia with colour blindness. J Peripher Nerv Syst. 2019;24:348–53.
78. Zhao Y, et al. A missense variant in AIFM1 caused mitochondrial dysfunction and intolerance to riboflavin deficiency. Neuromolecular Med. 2023;25:489–500.
79. Wang Q, Xingxing L, Ding Z, Qi Y, Liu Y. Whole exome sequencing identifies a novel variant in an apoptosis-inducing factor gene associated with X-linked recessive hearing loss in a Chinese family. Genet Mol Biol. 2019;42:543–8.
80. Rinaldi C, et al. Cowchock syndrome is associated with a mutation in Apoptosis-Inducing factor. Am J Hum Genet. 2012;91:1095–102.
81. Miyake N, et al. X-linked hypomyelination with spondylometaphyseal dysplasia (H-SMD) associated with mutations in AIFM1. Neurogenetics. 2017;18:185–94.

82. Pandolfo M, Rai M, Remiche G, Desmyter L, Vandernoot I. Cerebellar ataxia, neuropathy, hearing loss, and intellectual disability due to AIFM1 mutation. Neurol Genet. 2020;6:e420.
83. Kawarai T, et al. A novel AIFM1 missense mutation in a Japanese patient with ataxic sensory neuronopathy and hearing impairment. J Neurol Sci. 2020;409:116584.
84. Pronicka E, et al. New perspective in diagnostics of mitochondrial disorders: two years' experience with whole-exome sequencing at a National paediatric centre. J Transl Med. 2016;14:174.
85. Moss T, et al. Severe multisystem pathology, metabolic acidosis, mitochondrial dysfunction, and early death associated with an X-linked AIFM1 variant. Cold Spring Harb Mol Case Stud. 2021;7:a006081.
86. Mierzewska H, et al. Spondyloepimetaphyseal dysplasia with neurodegeneration associated with AIFM1 mutation - a novel phenotype of the mitochondrial disease. Clin Genet. 2017;91:30–7.
87. Wang H et al. High Frequency of AIFM1 Variants and Phenotype Progression of Auditory Neuropathy in a Chinese Population. *Neural Plast* 2020, 5625768 (2020).
88. Jeong EG, et al. Immunohistochemical and mutational analysis of apoptosis-inducing factor (AIF) in colorectal carcinomas. APMIS. 2006;114:867–73.
89. Fan T, et al. Implications of Bit1 and AIF overexpressions in esophageal squamous cell carcinoma. Tumour Biol. 2014;35:519–27.
90. Lee JW, et al. Immunohistochemical analysis of apoptosis-inducing factor (AIF) expression in gastric carcinomas. Pathol Res Pract. 2006;202:497–501.
91. Lewis EM, et al. The enzymatic activity of Apoptosis-inducing factor supports energy metabolism benefiting the growth and invasiveness of advanced prostate Cancer cells. J Biol Chem. 2012;287:43862–75.
92. Rao S, et al. AIF-regulated oxidative phosphorylation supports lung cancer development. Cell Res. 2019;29:579–91.
93. Scott AJ, Wilkinson AS, Wilkinson JC. Basal metabolic state governs AIF-dependent growth support in pancreatic cancer cells. BMC Cancer. 2016;16:286.
94. Skyrlas A, et al. Expression of apoptosis-inducing factor (AIF) in keratoacanthomas and squamous cell carcinomas of the skin. Exp Dermatol. 2011;20:674–6.
95. Zou R, Zhao W, Xiao S, Lu Y. A signature of three Apoptosis-Related genes predicts overall survival in breast Cancer. Front Surg. 2022;9:863035.
96. Cangelosi D, et al. Hypoxia predicts poor prognosis in neuroblastoma patients and associates with biological mechanisms involved in telomerase activation and tumor microenvironment reprogramming. Cancers (Basel). 2020;12:2343.
97. Su Z, et al. An investigation of biomarkers derived from legacy microarray data for their utility in the RNA-seq era. Genome Biol. 2014;15:523.
98. Kocak H, et al. Hox-C9 activates the intrinsic pathway of apoptosis and is associated with spontaneous regression in neuroblastoma. Cell Death Dis. 2013;4:e586.
99. Oberthuer A, et al. Customized oligonucleotide microarray gene expression-based classification of neuroblastoma patients outperforms current clinical risk stratification. J Clin Oncol. 2006;24:5070–8.
100. Rajbhandari P, et al. Cross-Cohort analysis identifies a TEAD4-MYCN positive feedback loop as the core regulatory element of High-Risk neuroblastoma. Cancer Discov. 2018;8:582–99.
101. Molenaar JJ, et al. Sequencing of neuroblastoma identifies chromothripsis and defects in neuritogenesis genes. Nature. 2012;483:589–93.
102. Wang Q, et al. Integrative genomics identifies distinct molecular classes of neuroblastoma and shows that multiple genes are targeted by regional alterations in DNA copy number. Cancer Res. 2006;66:6050–62.
103. Hartlieb SA, et al. Alternative lengthening of telomeres in childhood neuroblastoma from genome to proteome. Nat Commun. 2021;12:1269.
104. Cancer Genome Atlas Research Network. The molecular taxonomy of primary prostate Cancer. Cell. 2015;163:1011–25.
105. Bogunovic D, et al. Immune profile and mitotic index of metastatic melanoma lesions enhance clinical staging in predicting patient survival. Proc Natl Acad Sci U S A. 2009;106:20429–34.
106. Yamauchi M, et al. Epidermal growth factor receptor tyrosine kinase defines critical prognostic genes of stage I lung adenocarcinoma. PLoS ONE. 2012;7:e43923.
107. Okayama H, et al. Identification of genes upregulated in ALK-positive and EGFR/KRAS/ALK-negative lung adenocarcinomas. Cancer Res. 2012;72:100–11.
108. Pawitan Y, et al. Gene expression profiling spares early breast cancer patients from adjuvant therapy: derived and validated in two population-based cohorts. Breast Cancer Res. 2005;7:R953–964.
109. Cancer Genome Atlas Network. Genomic classification of cutaneous melanoma. Cell. 2015;161:1681–96.
110. Davis CF, et al. The somatic genomic landscape of chromophobe renal cell carcinoma. Cancer Cell. 2014;26:319–30.
111. Cardesa-Salzmann TM, et al. High microvessel density determines a poor outcome in patients with diffuse large B-cell lymphoma treated with rituximab plus chemotherapy. Haematologica. 2011;96:996–1001.
112. Cancer Genome Atlas Research Network. Integrated genomic characterization of oesophageal carcinoma. Nature. 2017;541:169–75.
113. Scott DW, et al. New molecular assay for the proliferation signature in mantle cell lymphoma applicable to Formalin-Fixed Paraffin-Embedded biopsies. J Clin Oncol. 2017;35:1668–77.
114. Hanamura I, Huang Y, Zhan F, Barlogie B, Shaughnessy J. Prognostic value of Cyclin D2 mRNA expression in newly diagnosed multiple myeloma treated with high-dose chemotherapy and tandem autologous stem cell transplantations. Leukemia. 2006;20:1288–90.
115. Asgharzadeh S, et al. Prognostic significance of gene expression profiles of metastatic neuroblastomas lacking MYCN gene amplification. J Natl Cancer Inst. 2006;98:1193–203.
116. Bild AH, et al. Oncogenic pathway signatures in human cancers as a guide to targeted therapies. Nature. 2006;439:353–7.
117. Gadd S, et al. A children's oncology group and TARGET initiative exploring the genetic landscape of Wilms tumor. Nat Genet. 2017;49:1487–94.
118. Selvanathan SP, et al. Oncogenic fusion protein EWS-FLI1 is a network hub that regulates alternative splicing. Proc Natl Acad Sci U S A. 2015;112:E1307–1316.
119. Cirenajwis H, et al. Molecular stratification of metastatic melanoma using gene expression profiling: prediction of survival outcome and benefit from molecular targeted therapy. Oncotarget. 2015;6:12297–309.
120. Robertson AG, et al. Integrative analysis identifies four molecular and clinical subsets in uveal melanoma. Cancer Cell. 2017;32:204–e22015.
121. Williamson D, et al. Medulloblastoma group 3 and 4 tumors comprise a clinically and biologically significant expression continuum reflecting human cerebellar development. Cell Rep. 2022;40:111162.
122. Cavalli FMG, et al. Intertumoral heterogeneity within Medulloblastoma subgroups. Cancer Cell. 2017;31:737–e7546.
123. Paugh BS, et al. Integrated molecular genetic profiling of pediatric high-grade gliomas reveals key differences with the adult disease. J Clin Oncol. 2010;28:3061–8.
124. Liu F, et al. PEG10 amplification at 7q21.3 potentiates large-cell transformation in cutaneous T-cell lymphoma. Blood. 2022;139:554–71.
125. Liu X, et al. Single-cell transcriptomics links malignant T cells to the tumor immune landscape in cutaneous T cell lymphoma. Nat Commun. 2022;13:1158.
126. Lai P, Liu F, Liu X, Sun J, Wang Y. Differential molecular programs of cutaneous anaplastic large cell lymphoma and CD30-positive transformed mycosis fungoides. Front Immunol. 2023;14:1270365.
127. Tran HC, et al. TGFβR1 Blockade with Galunisertib (LY2157299) enhances Anti-Neuroblastoma activity of Anti-GD2 antibody Dinutuximab (ch14.18) with natural killer cells. Clin Cancer Res. 2017;23:804–13.
128. Cherniack AD, et al. Integrated molecular characterization of uterine carcinosarcoma. Cancer Cell. 2017;31:411–23.
129. Vogel MJ, et al. FOXO1 repression contributes to block of plasma cell differentiation in classical hodgkin lymphoma. Blood. 2014;124:3118–29.
130. Iqbal J, et al. Gene expression signatures delineate biological and prognostic subgroups in peripheral T-cell lymphoma. Blood. 2014;123:2915–23.
131. Radovich M, et al. The integrated genomic landscape of thymic epithelial tumors. Cancer Cell. 2018;33:244–e25810.
132. Cancer Genome Atlas Research Network. Genomic and epigenomic landscapes of adult de Novo acute myeloid leukemia. N Engl J Med. 2013;368:2059–74.
133. Saintigny P, et al. Gene expression profiling predicts the development of oral cancer. Cancer Prev Res (Phila). 2011;4:218–29.
134. Zheng S, et al. Comprehensive Pan-Genomic characterization of adrenocortical carcinoma. Cancer Cell. 2016;29:723–36.
135. Nunes L, et al. Prognostic genome and transcriptome signatures in colorectal cancers. Nature. 2024;633:137–46.
136. Creighton CJ, et al. Comprehensive molecular characterization of clear cell renal cell carcinoma. Nature. 2013;499:43–9.

137. Cancer Genome Atlas Research Network. Comprehensive molecular characterization of papillary Renal-Cell carcinoma. N Engl J Med. 2016;374:135–45.
138. Cancer Genome Atlas Research Network. Comprehensive genomic characterization defines human glioblastoma genes and core pathways. Nature. 2008;455:1061–8.
139. Oh SC, et al. Clinical and genomic landscape of gastric cancer with a mesenchymal phenotype. Nat Commun. 2018;9:1777.
140. Guinney J, et al. The consensus molecular subtypes of colorectal cancer. Nat Med. 2015;21:1350–6.
141. Stratford JK, et al. A six-gene signature predicts survival of patients with localized pancreatic ductal adenocarcinoma. PLoS Med. 2010;7:e1000307.
142. Bailey P, et al. Genomic analyses identify molecular subtypes of pancreatic cancer. Nature. 2016;531:47–52.
143. Mateescu B, et al. miR-141 and miR-200a act on ovarian tumorigenesis by controlling oxidative stress response. Nat Med. 2011;17:1627–35.
144. Cancer Genome Atlas Research Network. Electronic address: andrew_aguirre@dfci.harvard.edu & Cancer genome atlas research network. Integrated genomic characterization of pancreatic ductal adenocarcinoma. Cancer Cell. 2017;32:185–e20313.
145. Hmeljak J, et al. Integrative molecular characterization of malignant pleural mesothelioma. Cancer Discov. 2018;8:1548–65.
146. Lisowska KM, et al. Gene expression analysis in ovarian cancer - faults and hints from DNA microarray study. Front Oncol. 2014;4:6.
147. Hagemann S, et al. IGF2BP1 induces neuroblastoma via a druggable feed-forward loop with MYCN promoting 17q oncogene expression. Mol Cancer. 2023;22:88.
148. Cancer Genome Atlas Research Network. Integrated genomic analyses of ovarian carcinoma. Nature. 2011;474:609–15.
149. Emons G, et al. Gene-expression profiles of pretreatment biopsies predict complete response of rectal cancer patients to preoperative chemoradiotherapy. Br J Cancer. 2022;127:766–75.
150. Cao L, et al. Proteogenomic characterization of pancreatic ductal adenocarcinoma. Cell. 2021;184:5031–e505226.
151. Clay MR, et al. Methylation profiling reveals novel molecular classes of rhabdomyosarcoma. Sci Rep. 2021;11:22213.

Publisher's note